

# Implications of DFN Model Selection in Open Pit Bench Stability Analyses

Martin Grenon<sup>(1)</sup> and John Hadjigeorgiou<sup>(2)</sup>

(1) Département de génie des mines, de la métallurgie et des matériaux  
Faculté des sciences et de génie, Université Laval  
Pavillon Adrien-Pouliot, 1065, avenue de la Médecine  
Québec (Québec) G1V 0A6 Canada.

(2) Pierre Lassonde Chair in Mining Engineering, University of Toronto  
Lassonde Mining Building, 170 College Street, Room 119A  
Toronto, Ontario, Canada, M5S 3E3.martin.grenon@gmn.ulaval.ca; John.Hadjigeorgiou@utoronto.ca

## ABSTRACT

A coupled Discrete Fracture Network (DFN) – Limit Equilibrium Analysis (LEA) approach to the design of bench face slopes in open pit mines has significant advantages over conventional analyses. The reliability of this approach is directly related to the quality of the input data and the ability for the generated DFN to adequately capture the characteristics of the rock mass. Different DFN model generators have specific input requirements and inherent assumptions. This paper addresses the critical issue of selecting an appropriate DFN model. Through a worked example, it illustrates the implications of selecting a series of different DFN models and generators on the stability analyses, and interpretation of the results. This is shown to have significant impact on the design of open pit slopes.

Keywords: bench face stability, Discrete Fracture Network (DFN), Limit Equilibrium Analysis (LEA).

## ***Implicaciones de la selección del modelo DFN en el análisis de estabilidad de bancos a cielo abierto***

### RESUMEN

*En el diseño de estabilidad de laderas de bancos en minas a cielo abierto, un enfoque que acopla la Malla de Fracturas Discretas (DFN) y el Análisis de Equilibrio Límite (LEA) tiene ventajas significativas sobre un análisis convencional. La fiabilidad de este enfoque está directamente relacionado a la calidad de los datos de entrada y a la habilidad para la generación de la DFN que capture adecuadamente las características del macizo rocoso. Distintos generadores de DFN tienen requerimientos específicos de entrada y asunciones inherentes a los mismos. Este trabajo trata sobre el problema crítico de seleccionar el modelo apropiado de DFN. A través de un ejemplo elaborado se ilustran las implicaciones de seleccionar una serie de diferentes modelos y generadores DFN sobre el análisis de estabilidad e interpretación de los resultados. Se muestra como este factor tiene un impacto significativo sobre el diseño de las pendientes a cielo abierto.*

*Palabras clave: estabilidad de laderas de bancos, Malla de fracturas Discretas (DFN), Análisis de Equilibrio Límite (LEA).*

**Introduction**

A comprehensive slope management programme in an open pit mine should address stability issues at the bench, inter-ramp and overall or global scale. Bench stability is controlled mainly by local geological structure, whereas inter-ramp stability is controlled by both local small scale and regional geological features such as faults and contacts. At the global slope level, stability is controlled by both the rock mass properties and large geological features.

Recent years have seen considerable advancements in data collection techniques to provide the necessary input parameters for slope stability analyses and monitoring the performance of slopes. Furthermore, there is a greater access to sophisticated numerical tools, including discrete fractures networks

(DFN), 3D limit equilibrium and 3D stress analyses numerical models to undertake comprehensive stability analyses, Jing (2003). The limitations of these powerful tools and their inherent assumptions, however, are not always understood or documented. This paper focuses on the use of DFN models and limit equilibrium tools, for stability analyses at the bench scale for an open pit hard rock mine. The emphasis is on an understanding of the consequences and interpretation of using different DFN models on the slope stability analyses.

**Discrete Fracture Networks (DFN)**

A comprehensive geotechnical model for slope stability analyses and management includes information on material distribution, structural anisotropy, strength

DFN Model	Description	Geometric parameters to generate DFN
<b>Baecher Model</b> (Baecher et al 1978)	The model assumes a circular fracture shape. Fracture centres are located uniformly in space, using a Poisson process and fractures are generated as disks with a given radius and orientation. Fractures terminate in intact rock and intersect each other. Any combination of fracture size, location, and orientation assumptions are possible.	Density of the fractures (number of fractures per unit volume), the orientation distribution of these fractures, the size and shape of the fractures.
<b>Enhanced Baecher Model</b> (Geier et al 1988)	Can account for fracture termination at intersections with pre-existing fractures. It can employ the concept of termination probability (the probability that a fracture of a given set will terminate when it intersects a fracture of an earlier set). The model can accommodate more general fracture shapes ( defined by polygons)	Density of the fractures (number of fractures per unit volume), the orientation distribution of these fractures, the size and shape of the fractures.
<b>Baecher Algorithm, Revised Terminations (BART) Model</b> (Dershowitz et al, 1998)	Capable of generating non-uniform fracture locations. The basic difference from the Enhanced Baecher Model is the way it treats fracture termination modes. The additional input of termination percentage can provide a better correlation to field data than other variations of the Baecher model. As the locations of secondary fractures are controlled by the locations of the primary fractures, the resulting fracture populations exhibit spatial correlation and tend to occur in clusters or chains.	Density of the fractures (number of fractures per unit volume), the orientation distribution of these fractures, the size and shape of the fractures. Termination is assigned by termination percentage: the percentage of fractures that terminate at intersections with other fractures.
<b>Nearest Neighbour Model</b> (Dershowitz et al 1998)	The Nearest Neighbour model is a semi-stochastic, pattern-based model. It differs from the Enhanced Baecher model in the way it manages the spatial distribution of fractures. It is capable of simulating fractures clustered around major points and faults by preferentially producing new fractures in the vicinity of earlier fractures. This is achieved by organising and generating fractures in sequence into primary, secondary and tertiary groups. Fractures in the primary groups dominate the generation of fractures in succeeding groups. The probability of a fracture at a point x in three-dimensional space is given by: $P_x(x) = CL^{-b} \quad (1)$ Where L is the distance from point x to the nearest fracture of a previous, dominant group, and b and C are empirical constants.	Density of the fractures (number of fractures per unit volume), the orientation distribution of these fractures, the size and shape of the fractures. Termination is assigned by termination percentage: the percentage of fractures that terminate at intersections with other fractures. Data on the spatial interrelationship of the fractures. The Nearest Neighbour Model can also use the termination probability.
<b>Veneziano Model</b> (Veneziano, 1978)	Relies on the generation of a Poisson network of planes in 3D space followed by a secondary process of tessellation by a Poisson line process and marking of polygonal areas. A portion of these polygons is randomly marked as jointed, while the remainder is defined as intact rock. Veneziano model is similar to the Baecher model with the exception that fractures are represented by coplanar line segments. Use of the Veneziano model results in an exponential distribution of fracture trace lengths, rather than lognormal distribution as generated in the Baecher model.	Density of the fractures (number of fractures per unit volume), the orientation distribution of these fractures, the size and shape of the fractures.

**Table 1.** DFN models, modified from Staub et al (2002) and Grenon et al. (2017).

**Tabla 1.** Modelos DFN, modificado de Staub et al (2002) y Grenon et al. (2017).

parameters and hydrogeological factors, Guest and Read (2009). A geotechnical structural domain is a volume of rock having similar discontinuity spatial, and specific associated structural characteristics, Mathis (2016). The use of Discrete Fracture Networks (DFN) to successfully represent the structural domain is dependent on the following tasks:

- The collection of adequate and quality input data
- Understanding the impact of the choice of employed DFN model on the analysis
- Interpretation and understanding of the significance of the results

The data collection requirements for constructing representative DFN models has been discussed to some length in several publications, e.g. Elmoutie and Poropat (2011), Hadjigeorgiou (2012), Elmo et al (2014). The interpretation and understanding of results, however, is often limited to establishing an adequate number of DFN simulations with the impact of the choice of DFN model, receiving less attention. This is somewhat surprising given the inherent differences and assumptions of the various DFN models. In particular the various DFN software generators have access to different algorithms and quite often there is little information, in the published literature, what model was used. Table 1 provides a summary description of DFN models implemented in the Fracture-SG software package (Grenon and Hadjigeorgiou, 2018) and used for this investigation.

**Open Pit Case Study**

The significance of the choice of DFN model on the stability analysis and interpretation is illustrated using a worked example for an open pit mine. The objective was to generate a series of DFN models, identify all structurally defined wedges, and undertake a series of limit equilibrium analyses at the bench scale. All generated DFN models were in the same geotechnical structural domain defined by the major fracture sets shown in Figure 1. The input parameters (fracture mean orientation and dispersion around mean value), to generate the DFN models are summarised in Table

2. In a DFN generator, fracture size can be represented by fracture trace length or area and fracture intensity is determined from fracture spacing, fracture intensity  $P_{21}$  and  $P_{32}$  as outlined by Dershowitz and Herda (1992). To facilitate the stability analyses all fracture set were assigned an angle of friction of 30° and no cohesion.

**Generated DFN models**

A series of DFN models were generated using the Fracture-SG software package, Grenon and Hadjigeorgiou (2018). All generated models, based on the Enhanced Baecher, BART, Nearest Neighbour and Veneziano algorithms, and were calibrated using the two-sample Kolmogorov-Smirnov test (KS). The KS procedure returns a test decision for the null hypothesis that the data are from the same continuous distribution. All generated DFN models were deemed representative of the same rock mass conditions.

In this investigation a more rigorous calibration process was implemented than typically reported in the technical literature. The interest in this work was to further assess the implications of using specific features of the models, e.g. fracture termination, set hierarchy or co-planarity. As summarised in Table 1, it is these features that contribute to the intrinsic characteristics of the resulting DFN simulations. In this context the objective was not to match or represent field conditions in a particular rock mass but to investigate their potential impact on the generated wedges along the slope bench and identify potential instabilities.

The different algorithms required a series of assumptions. For example, the Baecher model DFN considered by default fracture termination in intact rock. The BART Model was generated with fracture sets 2, 3, and 4 having a 100% termination in set 1, i.e. systematically creating connecting fractures. The generated Nearest Neighbour model identified fracture set 1 as the primary set while the three other sets were secondary to set 1. This resulted in creating fracture clusters around set 1. In this case, generated fractures terminated in intact rock and a “b” value of 2 and a “C” value of 1 were assigned to the three fracture sets. It

Fracture Set	1	2	3	4
Mean dip (°)/dip direction (°)	06/056	47/135	45/090	67/024
Fisher’s K constant	52	29	58	16
Mean Trace length (m)	12.0	4.0	3.5	3.0
$P_{21}$	5.94	2.34	1.2	1

**Table 2.** Typical Discrete Fracture Network input parameters.  
**Tabla 2.** Parámetros de entrada típicos para la Malla de Fracturas Discretas.

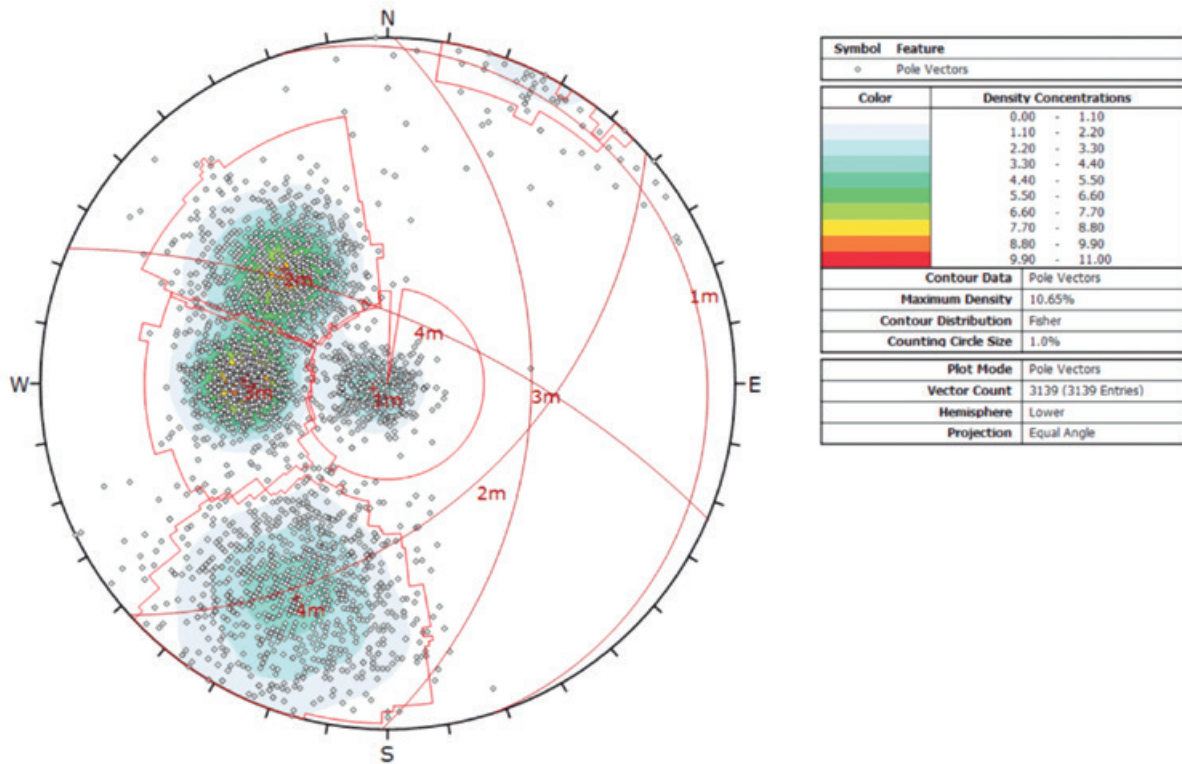


**Figure 1.** Stereonet projection of the four sets defining the input parameters.

**Figure 1.** Proyección estereográfica de los cuatro conjuntos que definen los parámetros de entrada.

has already been discussed that the Veneziano model intrinsically considers coplanar fractures.

The same validation procedure was used for all fracture sets in all employed models (Enhanced Baecher, BART, NNM, and Veneziano). To illustrate the process, the methodology is described using fracture set 1 of the Enhanced Baecher Model. In all models seven sampling scan planes were introduced within the simulation volume. The sampling scan planes had the same orientation as rock exposures that could be mapped in-situ. 100 circular sampling windows were randomly assigned on every scan plane to collect the structural data used in the calibration process.

The DFN-Enhanced-Baecher generated data for fracture set 1 were defined by a mean orientation of  $06^\circ/056^\circ$  and a K of 52. These values are consistent with the field data reported in Table 1. The methodology proposed by Fisher et al. (1993) was used to compare the mean value and dispersion modelled to the available field data. A Student hypothesis test (alpha 5%) was used to compare the mean orientation resulting in a P value of 0.99. Consequently, it was not possible to reject the null hypothesis that the two values are statistically equal. A Fisher hypothesis test (alpha 5%) compared the dispersion around the mean value

resulted in a P value of 0.40 and did not allow the rejection of the null hypothesis.

The approach by Zhang and Einstein (1998) was used to analyse the trace length data yielding in an unbiased mean trace length of 12.0 m. The distribution of the traces intercepted by the sampling window indicated a standard deviation of 0.89 and was best represented by a log normal distribution. The unbiased mean trace length was evaluated based on the 100 sampling windows obtaining a value of 12.1 m which was comparable to the input value. The trace length was determined for all fractures intercepting the sampling windows within the Enhanced Baecher DFN. The distributive nature of the modelled and field data were compared using a KS-test for two samples. The resulting P-value of 0.82 suggested that it was not possible to reject the null hypothesis that these two samples are statistically similarly distributed.

Input data for  $P_{21}$  had a value of 5.94 with an average  $P_{21}$  value, based on the 100 sampling windows of 5.89. The standard deviation of 0.33 for  $P_{21}$ , based on the 100 sampling windows, suggests some variability in the results. This comprehensive and rigorous approach was used to calibrate the fracture set properties for all sets for all the DFN models used in this paper.



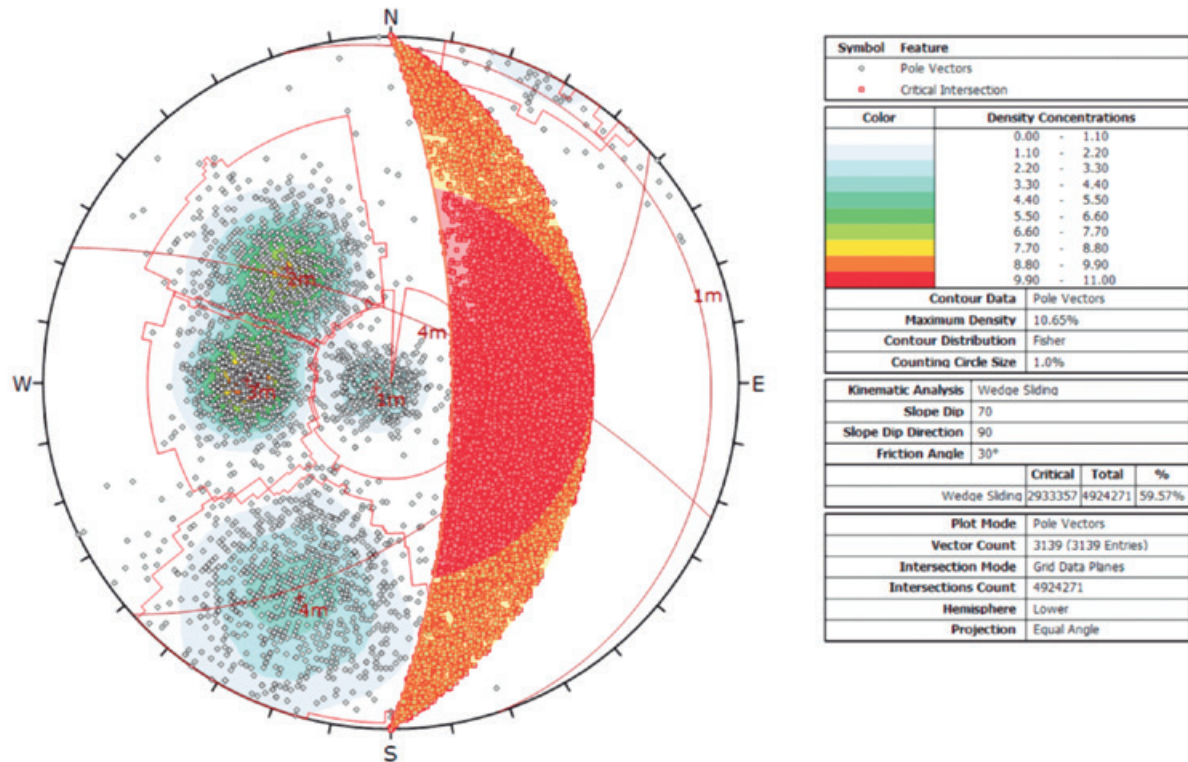


**Figure 2.** Kinematic analysis for the worked example.  
**Figura 2.** Análisis cinemático para el ejemplo elaborado.

### Slope Stability Analyses

There are several tools for analysing the stability of bench slopes susceptible to wedge failure. The benefits of a combined DFN-LEA analyses for slope stability has been identified by Dershowitz and Carvalho (1996). Grenon and Hadjigeorgiou (2008, 2012) employed DFN-LEA for the stability of several rock slopes along road embankments. Mathis (2014) compared the different tools for predicting bench face angles and their associated reliability distributions, concluding that, DFN based techniques are better predictors of bench stability, provided appropriate input parameters to construct and test the DFN models are used. Recently, Rogers et al (2018) employed DFN based tools for developing bench face angle criteria for an open pit mine suggesting that among other advantages they provide a clear auditable route from data acquisition to modelling and analysis.

### Kinematic and kinetic analyses

A kinematic analysis is normally the first stage in a rock slope investigation where the objective is to establish if a given slope geometry and fracture orientation combination will result in a kinematically feasible

wedge failure. A kinetic analysis indicates whether a kinematically feasible wedge will indeed move as a result of its low shearing resistance. In this investigation the rock mass was defined by the four fracture sets in Figure 1. The rock slope was inclined at 70/090. At its highest point, the bench slope is 15 m in height. The undertaken kinematic analysis illustrated in Figure 2 suggested that wedge failure is possible for a slope oriented at 70/090, along the intersection of fracture sets 2-3, 2-4, 3-4. Although this type of analysis can be used to determine the probability of sliding along these failure planes it cannot take into consideration the influence of fracture size and probability of occurrence. This is an important limitation.

### Deterministic and Probability of failure analyses

In practice, Limit Equilibrium Analyses are routinely used to evaluate the Factor of Safety (FoS) and Probability of Failure (PoF). The probability that any particular wedge is formed and susceptible to failure, can be quantified by employing a Monte-Carlo analysis. A statistical distribution is employed to define one or more parameters that control the stability of a given wedge. The probability of occurrence, however,

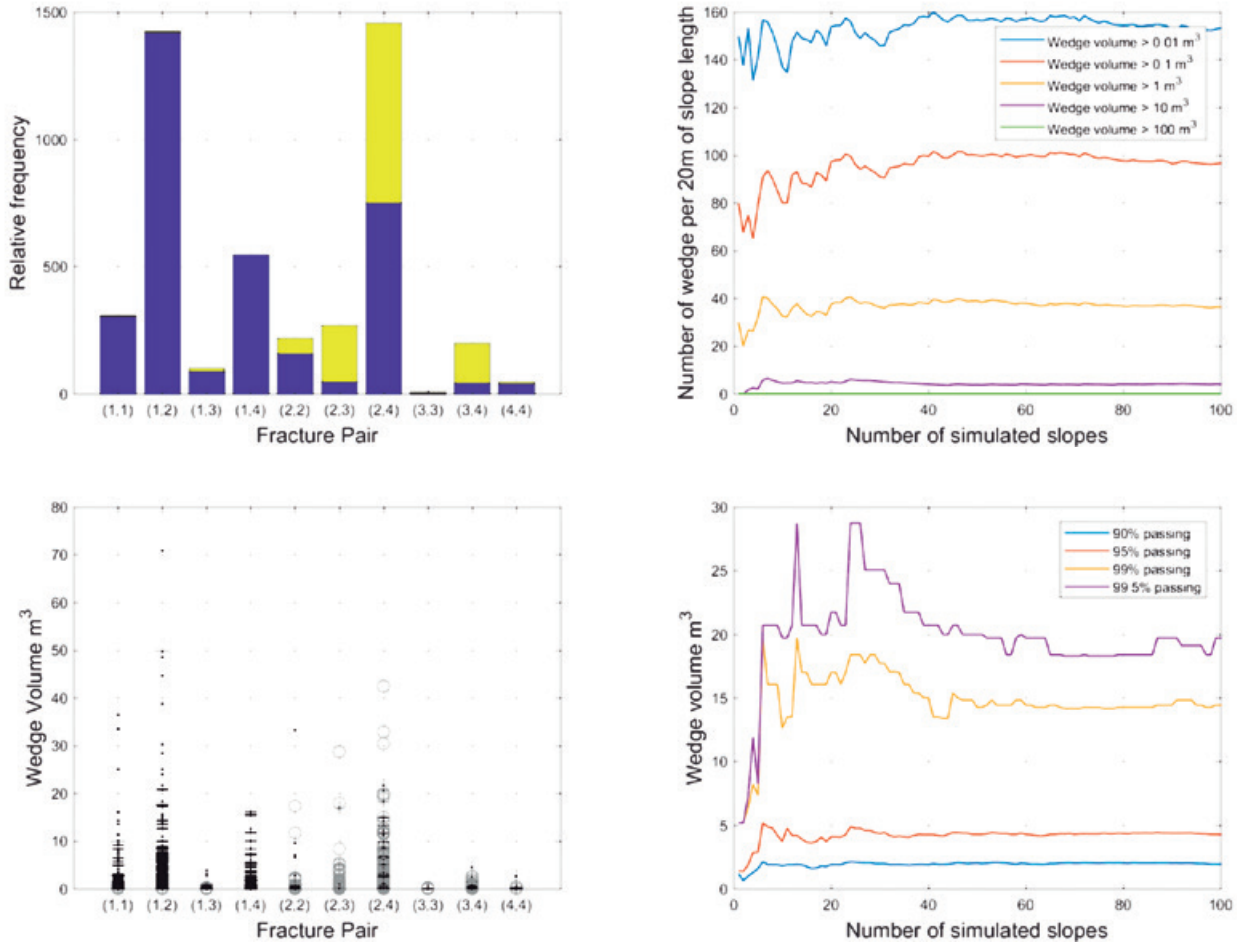


**Figure 3.** Baecher Batch simulation #1: 1- Histogram of the wedges formed at crest; 2- scatter plot of wedges volumes at crest (+ stable wedges, o unstable wedges); 3- Number of wedges per 20 m slope length; 4- Wedge at crest passing volumes.

**Figura 3.** Lote de Baecher simulación #1: 1- Histograma de las cuñas formadas en la cresta; 2- diagram de dispersión de los volúmenes de cuñas en la cresta (+ cuñas estables, o cuñas inestables); 3- Número de cuñas por 20 m de longitud de ladera; 4- Cuñas en los volúmenes de paso de cresta.

is difficult to assess as these approaches do not adequately address wedge instability size and frequency potential of wedge delineation along a given bench slope.

### Integrated DFN-LEA Approach

The integrated wedge-stability-DFN approach developed by Grenon and Hadjigeorgiou (2008) was used for the purposes of this investigation. The Fracture-SG code was used to create 100 DFN based on the Enhanced Baecher model. All generated fracture systems were 20 m x 20 m x 20 m in size. The inherent variability of structural properties was accounted for by selecting appropriate probability density function (pdf). In this study, fracture geometrical parameters

were defined by pdf, while material strength parameters were assigned deterministic values. The next step in this investigation involved the random introduction of slope localisations in every one of the 100 generated fracture systems. Along the crest of these geometrically identical slopes, more than 4000 wedges were created. The stability of every wedge formed at the crest of a slope was determined using limit equilibrium techniques implemented in the Fracture-SL code by Grenon and Hadjigeorgiou (2018).

The results of the integrated DFN-Wedge stability analyses for 100 DFN generated by the Enhanced Baecher model are summarised in Figure 3. It should be noted that given the model accounts for orientation variability, it is possible that wedges are also formed by fractures of the same set. These wedges are char-

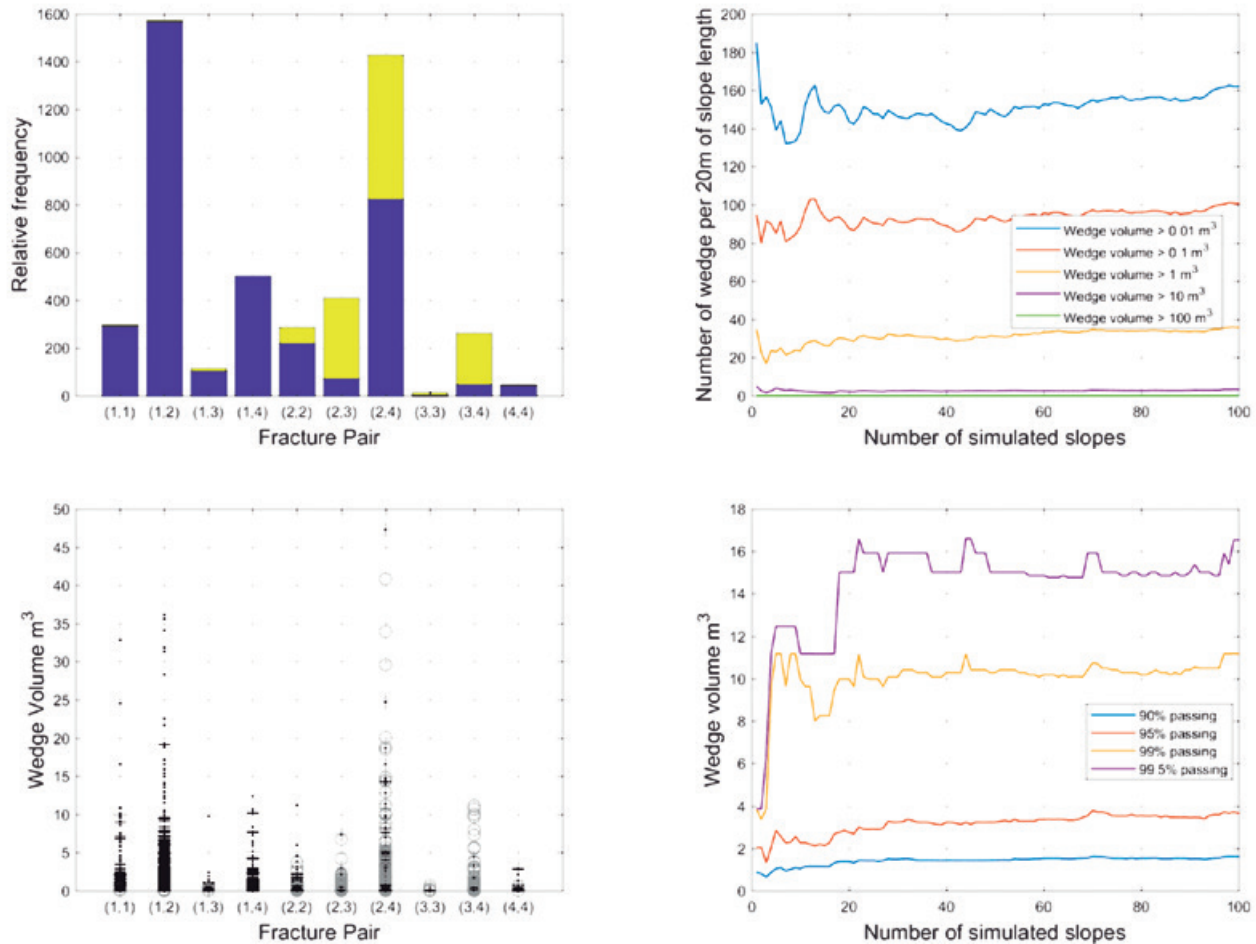


**Figure 4.** Baecher Batch simulation # 2: 1- Histogram of the wedges formed at crest; 2- scatter plot of wedges volumes at crest (+ stable wedges, o unstable wedges); 3- Number of wedges per 20 m slope length; 4- Wedge at crest passing volumes.

**Figura 4.** Lote de Baecher simulación #2: 1- Histograma de las cuñas formadas en la cresta; 2- diagram de dispersión de los volúmenes de cuñas en la cresta (+ cuñas estables, o cuñas inestables); 3- Número de cuñas por 20 m de longitud de ladera; 4- Cuñas en los volúmenes de paso de cresta.

acterised by an elongated shape and only a very small percentage of these wedges are unstable, as shown in the histogram in Figure 3-1. The most dominant set combinations in creating wedges are (1,2 and 2,4) while all wedges created by the former are stable, the latter produces 40% of all unstable wedges. Potentially non-stable wedges are also delineated by fracture pairs (2,2), (2,3) and (3,4).

The DFN based approach is very well suited for a probabilistic assessment of wedge size. In effect it is wedge size that is most often critical from an engineering and operational perspective. The wedge size is determined using a scatter plot of wedge size versus fracture set combinations. Figure 3-2 reveals that the wedge volume is generally small and the scatter plot illustrates that the largest unstable wedge (40 m³) is associated with fracture pair (2,4).

The probability of occurrence was also investigated, Figure 3-3. Based on this analysis, along a 20 m of slope crest, 100 wedges larger than 0.1 m³ can be expected with 38 wedges greater than 1 m³ and one larger than 10 m³. This is valuable information that can be used to verify the reliability of the design and consequences of instability. In this analysis 40 and 60 DFN were necessary to obtain reproducible results.

The generated data render themselves to a more quantitative approach of predicting the wedge size along the crest of a slope. As shown in Figure 3-4 90% of generated wedges will be smaller than 1.8 m³, 95% smaller than 4 m³, and 99% smaller than 14 m³ and 99.5% smaller than 20 m³. Grenon and Hadjigeorgiou (2008) used this type of chart to develop site specific reliability criteria for rock slopes.

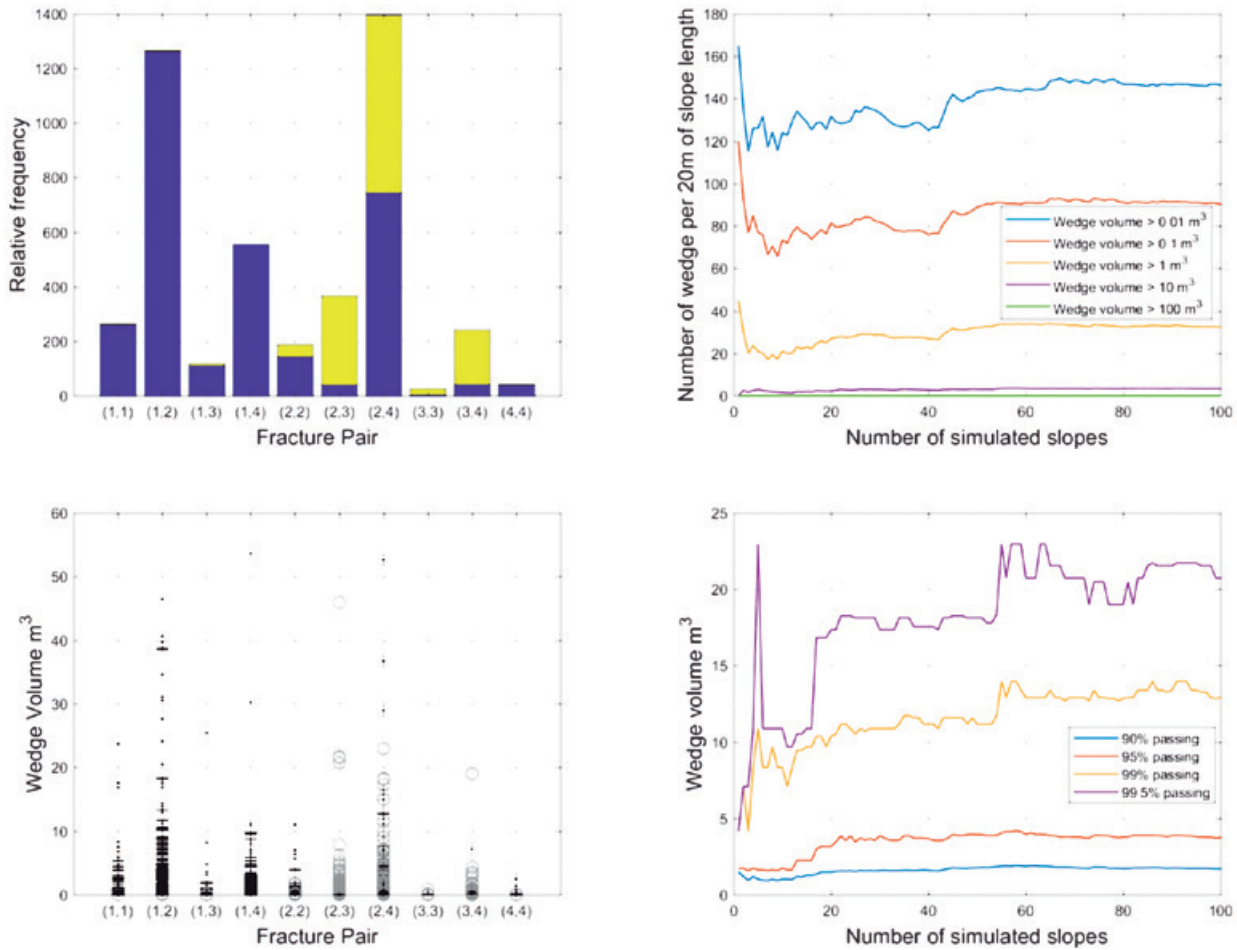


**Figure 5.** Baecher Batch simulation #3: 1- Histogram of the wedges formed at crest; 2- scatter plot of wedges volumes at crest (+ stable wedges, o unstable wedges); 3- Number of wedges per 20 m slope length; 4- Wedge at crest passing volumes.

**Figura 5.** Lote de Baecher simulación #5: 1- Histograma de las cuñas formadas en la cresta; 2- diagram de dispersión de los volúmenes de cuñas en la cresta (+ cuñas estables, o cuñas inestables); 3- Número de cuñas por 20 m de longitud de ladera; 4- Cuñas en los volúmenes de paso de cresta.

### Comparing Multiple Realisations of a Single Model (Repeatability)

A series of three batch analyses, each of 100 DFN, were generated to investigate the ability of a DFN model to produce similar wedge formation results along a 20 m long slope crest. As shown in Figures 3, 4, and 5 the total number of wedges and contributing fracture sets are quite similar. The proportion of unstable wedges remains constant. The maximum wedge volume is mostly associated with sets (2, 4) but for 1 series of DFN it is associated with combination (2, 3). The 99.5% passing was between 16 and 21 m<sup>3</sup>. The number of simulations to obtain consistent results is between 40

and 60 DFNs. The number of wedges formed, greater than 1 m<sup>3</sup>, is close to 40 per 20 m of slope crest. The process demonstrates that, in this case study, employing the Enhanced Baecher model resulted in repeatable results. This repeatability is important for design purposes. Once a number of simulations (realisations) demonstrate that a constant value is obtained for a given criterion, (e.g. number of 10 m<sup>3</sup> wedges) it is no longer necessary to perform further simulations. This is obviously time efficient and, once a constant value is obtained, it can be used with confidence for probabilistic design.

It is also important to note that due to the stochastic nature of DFN modelling, a certain variation in the



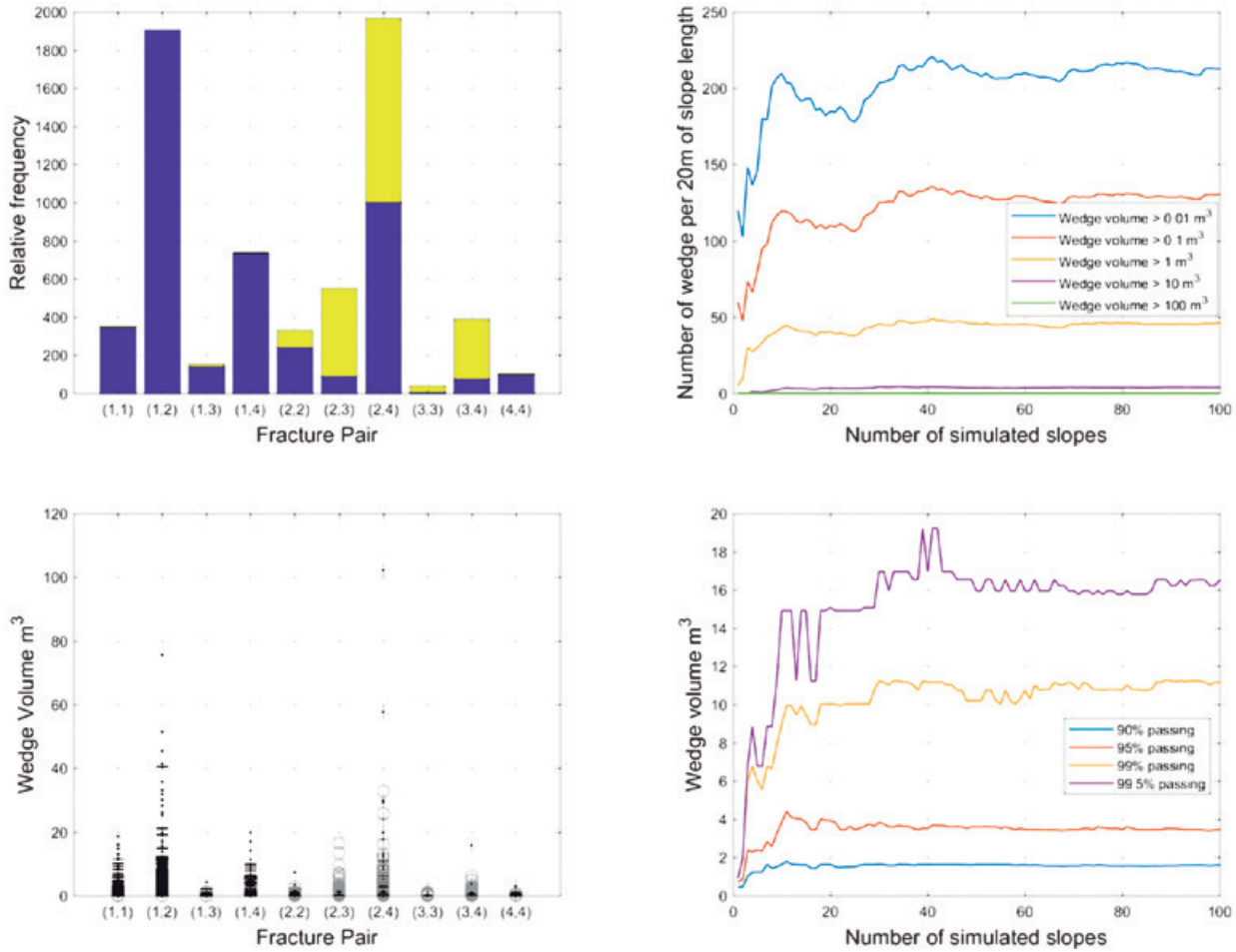


**Figure 6.** Bart Model: 1- Histogram of the wedges formed at crest; 2- scatter plot of wedges volumes at crest and; 3- Number of wedges per 20 m slope length; 4- Wedge at crest passing volumes.

**Figura 6.** Modelo de Bart: 1- Histograma de las cuñas formadas en la cresta; 2- diagram de dispersión de los volúmenes de cuñas en la cresta (+ cuñas estables, o cuñas inestables); 3- Número de cuñas por 20 m de longitud de ladera; 4- Cuñas en los volúmenes de paso de cresta.

results is to be expected. In practice a large number of simulations will tend to minimise these variations, Grenon and Hadjigeorgiou (2008). In the present work, the investigated parameter (wedge volume) reached a plateau after a certain number of simulations, Figures 3-4. In this context this is a reliable guide to select the desired number of simulations.

### Impact of DFN model choice

It is recognised that a successfully calibrated DFN can provide good statistical agreement with field data and increased confidence in subsequent slope stability analyses. This paper postulates that given the differences in the geometrical characteristics of DFN models, there can be significant influence on the analy-

sis and interpretation of the results of any stability analyses. This was investigated further by using the Enhanced Baecher, Bart, Nearest Neighbour and Veneziano algorithms to generate multiple DFN models. All DFN models were calibrated using the method described in section 3.

The quantitative results of these analyses are summarised in Figures 6 to 8. As illustrated in Figure 6, the BART generated DFN result in larger and more numerous wedges than the Baecher generated models in Figures 3 to 5. Using the BART algorithm resulted in 50 wedges of size greater than 1 m³ along the 20 m long slope. This implies that the model also resulted in a greater number of smaller wedges being delineated which was attributed to the fact that fractures are terminating along fractures of fracture set 1. As shown in

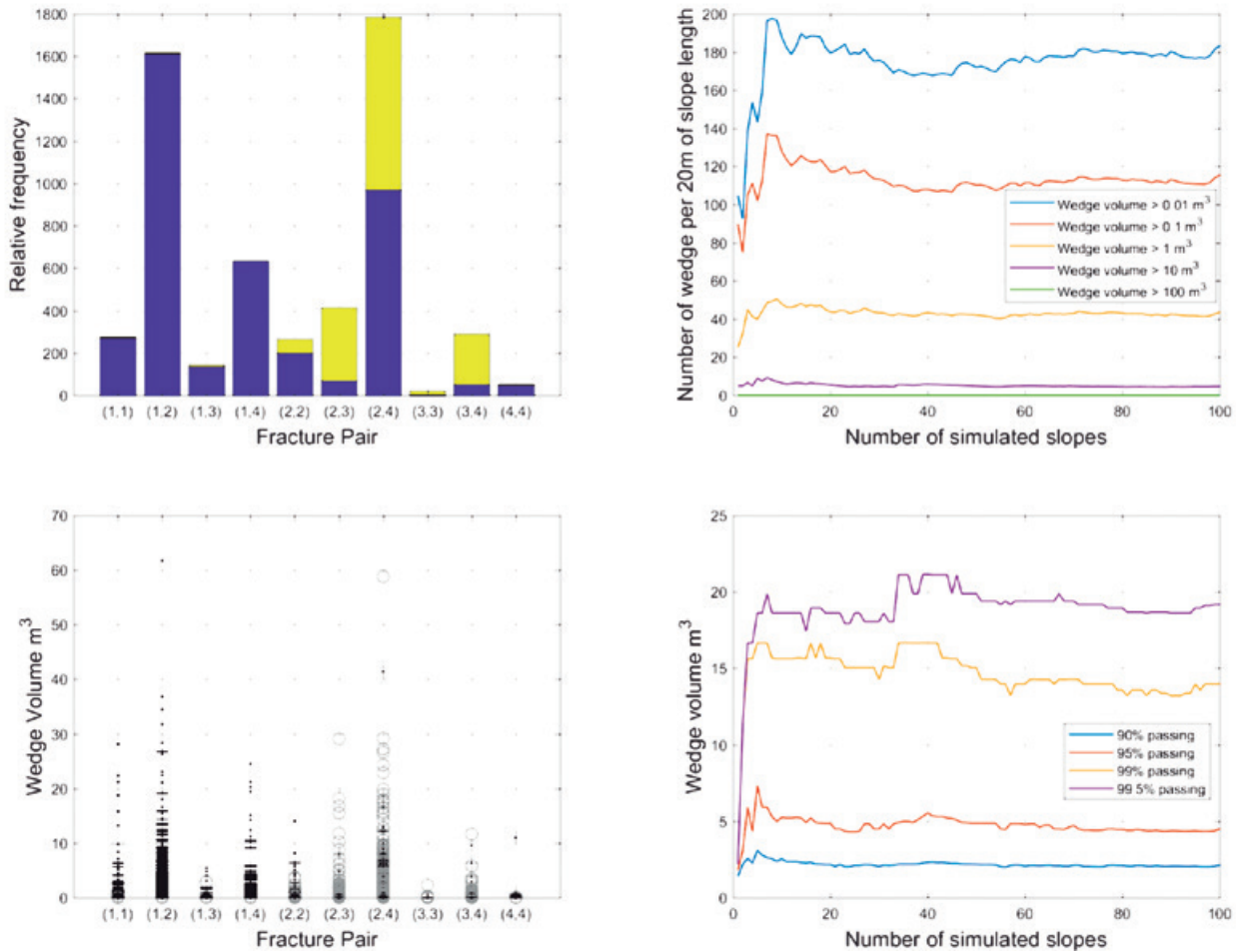


**Figure 7.** Nearest Neighbour Model: 1- Histogram of the wedges formed at crest; 2- scatter plot of wedges volumes at crest (+ stable wedges, o unstable wedges); 3- Number of wedges per 20 m slope length; 4- Wedge at crest passing volumes.  
**Figura 7.** Modelo de Vecino más Próximo: 1- Histograma de las cuñas formadas en la cresta; 2- diagram de dispersión de los volúmenes de cuñas en la cresta (+ cuñas estables, o cuñas inestables); 3- Número de cuñas por 20 m de longitud de ladera; 4- Cuñas en los volúmenes de paso de cresta.

Figure 7, Nearest Neighbour DFNs generated a greater number of wedges than the Enhanced Baecher model, albeit with a similar distribution. This follows from the formulation of the Nearest Neighbour method that groups fracture locally and consequently generate a greater number of wedges but with similar size distributions. Finally, the implementation of the Veneziano model resulted in a greater number of wedges that are smaller in size, Figure 8. This characteristic of the Veneziano model was previously observed in the formation of wedges in underground mining drifts, Grenon et al (2017). What these investigations clearly demonstrate is that the choice of DFN model can have significant impact on the results of any subsequent stability analyses.

Model selection should be based on the quality of field data and take into consideration all important as-

pects regarding the investigated problem. If joint clustering is important at a site for example it should be quantified and incorporated in the DFN passing analysis.

### Impact of Variations in Input Properties

Quite often in a mining project there are limited or insufficient data to perform comprehensive analyses. In certain cases there also may be a reluctance to invest in further data collection campaigns. This section reports on the potential impact on the analysis and design of bench slopes of an inherent variation in the required input properties, e.g. trace length and fracture intensity, to generate DFN models.

Two series of multiple DFNs were modelled. In the first series of simulations  $P_{32}$  was kept fixed while frac-

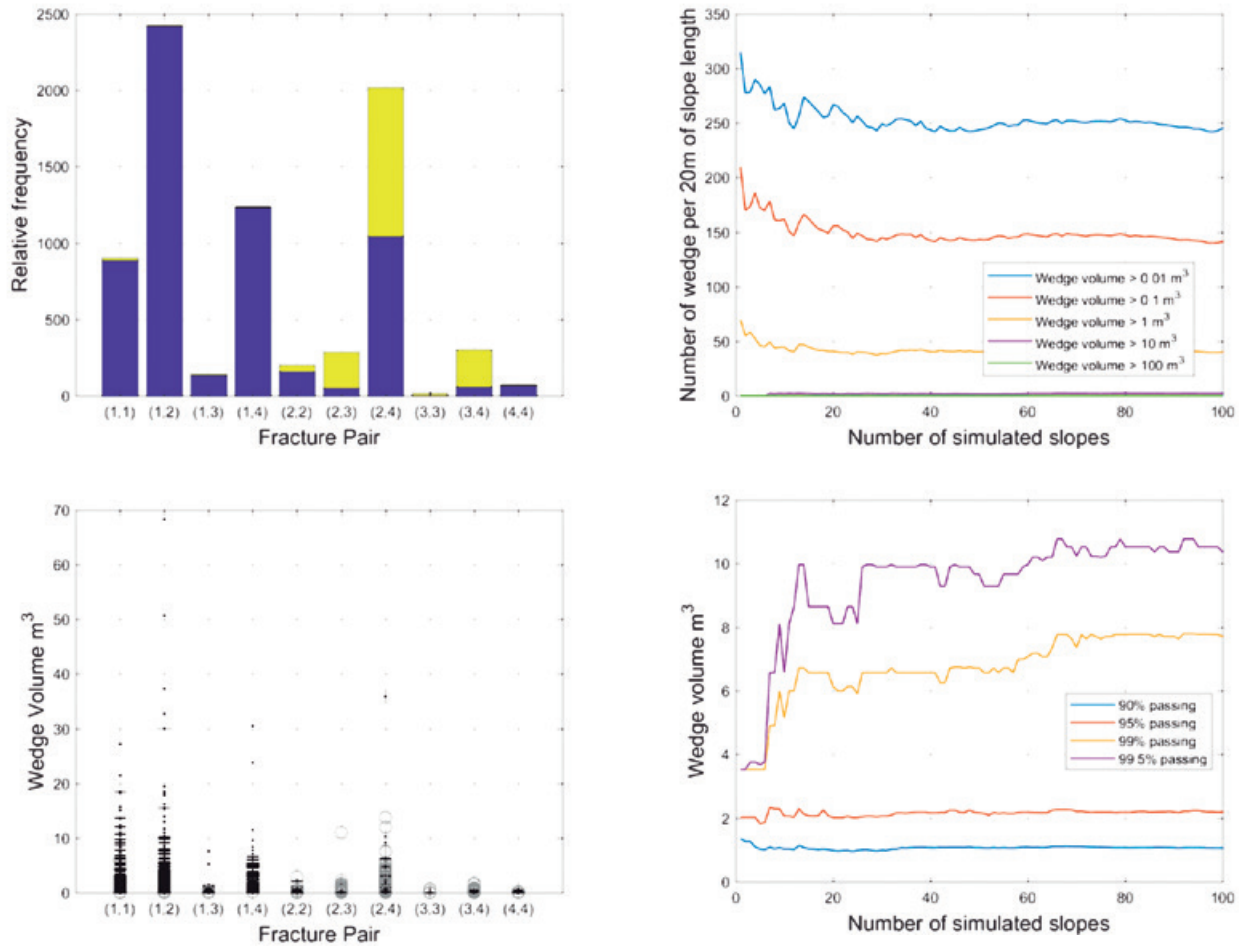


**Figure 8.** Veneziano Model: 1- Histogram of the wedges formed at crest; 2- scatter plot of wedges volumes at crest (+ stable wedges, o unstable wedges); 3- Number of wedges per 20 m slope length; 4- Wedge at crest passing volumes.

**Figura 8.** Modelo Veneciano: 1- Histograma de las cuñas formadas en la cresta; 2- diagram de dispersión de los volúmenes de cuñas en la cresta (+ cuñas estables, o cuñas inestables); 3- Número de cuñas por 20 m de longitud de ladera; 4- Cuñas en los volúmenes de paso de cresta.

ture size was at 10% of the initial mean value, Figure 9. The second series of tests kept the fracture area constant and used a  $P_{32}$  value ten times greater than the initial one, Figure 10.

In the first scenario, the same total fracture area ( $P_{32}$ ) defined the DFN compared to the initial DFN in Figure 3. The number of wedges formed by the combination of fracture sets (2,3); (2,4) and (3,4) was considerably smaller. A similar number of wedges was obtained from combination (1,2). The proportion of unstable versus stable wedge, and the probability of failure (PoF) was not different than the reference model. As a result of the reduction in fracture size, the size of the generated wedges decreased by a magnitude of 10. The smaller fracture size had a direct impact on the occurrence or creation of wedges

even if intensity ( $P_{32}$ ) remained unchanged. In this case 80 simulations were needed for the results to reach a representative plateau.

In the second scenario, a  $P_{32}$  value was selected, ten times the initial value used in Figure 3.

As shown in Figure 10 the number of wedges produced is roughly ten-fold the number reported for the Enhanced Baecher models in Figures 3 to 5. These results are consistent and in agreement with the greater fracture intensity of the models. The PoF remains similar to the initial findings. The greater number of fractures enables the creation of larger individual wedges, with some of them exceeding 150 m³. The size distribution of wedges remains similar to the initial scenarios: 99.5% of wedges are smaller than 20 m³; 95% smaller than 4 m³.

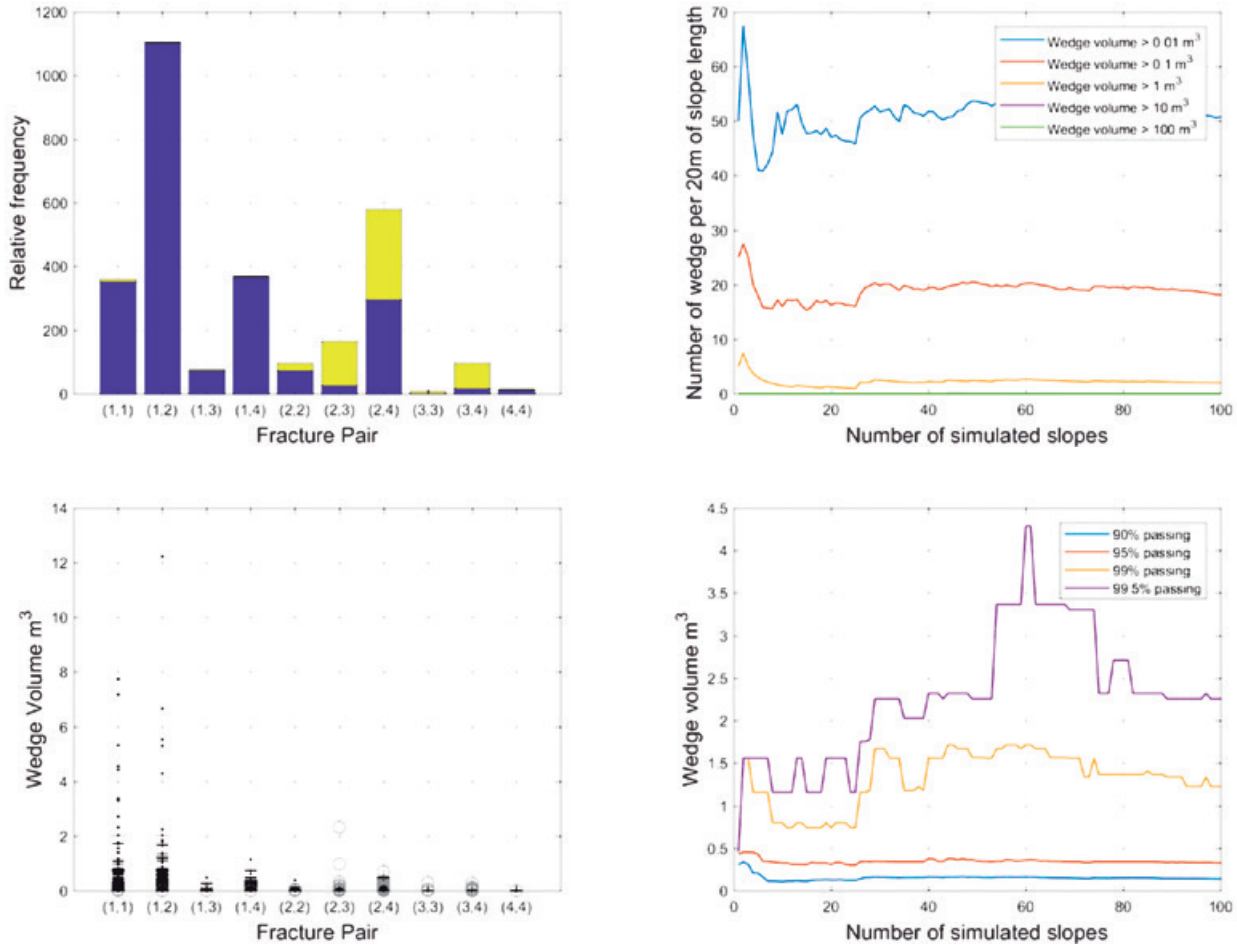


**Figure 9.** Enhanced Baecher Models with fractures defined by smaller areas and similar P32: 1- Histogram of the wedges formed at crest; 2- scatter plot of wedges volumes at crest (+ stable wedges, o unstable wedges); 3- Number of wedges per 20 m slope length; 4- Wedge at crest passing volumes.

**Figura 9.** Modelos de Baecher mejorados con fracturas definidas por áreas más pequeñas y similar P32: 1- Histograma de las cuñas formadas en la cresta; 2- diagram de dispersión de los volúmenes de cuñas en la cresta (+ cuñas estables, o cuñas inestables); 3- Número de cuñas por 20 m de longitud de ladera; 4- Cuñas en los volúmenes de paso de cresta.

This is consistent with the earlier investigations suggesting that increasing the fracture intensity does not have a significant impact on size distribution. On the other hand, the number of wedges increased ten-fold. The practical implication is that even though the wedge size distribution remains constant, the potential for slope instability along the bench is greater. Of further interest is that a plateau was reached after only 20 simulations. This may imply that the number of DFN simulations to obtain consistent results can vary depending on fracture intensity for a constant simulation volume.

## Conclusions

This paper addresses issues related to the choice of DFN generators for the analysis of the stability of bench slopes in open pit mines. It highlighted issues associated with the calibration process (fracture orientation, trace length and  $P_{21}$  distributions) between generated DFN models and field data. The emphasis in this investigation, however, is on the impact of the choice of DFN model in the generation of structurally defined wedges along a bench.

It was shown that multiple DFN realisations are essential to adequately represent the possible wedge formation



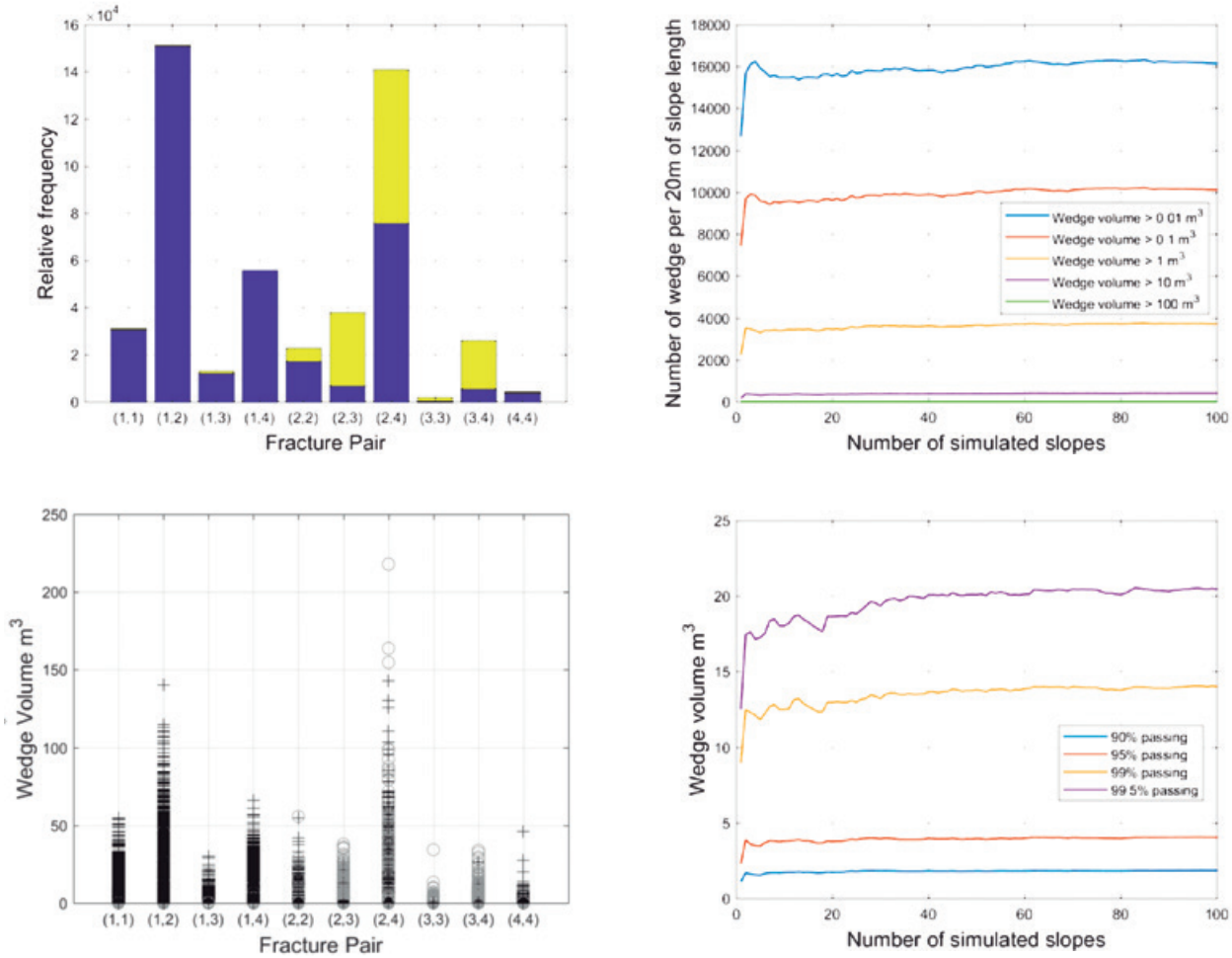


**Figure 10.** Enhanced Baecher Models with fractures defined by similar areas and larger P32: 1- Histogram of the wedges formed at crest; 2- scatter plot of wedges volumes at crest (+ stable wedges, o unstable wedges); 3- Number of wedges per 20 m slope length; 4- Wedge at crest passing volumes.

**Figura 10.** Modelos de Baecher mejorados con fracturas definidas por áreas similares y mayores P32: 1- Histograma de las cuñas formadas en la cresta; 2- diagram de dispersión de los volúmenes de cuñas en la cresta (+ cuñas estables, o cuñas inestables); 3- Número de cuñas por 20 m de longitud de ladera; 4- Cuñas en los volúmenes de paso de cresta.

along a slope crest. Consequently, the use of limited DFN although convenient may result in misleading results.

Although there is a significant degree of repeatability in the generated DFNs from a specific model there are important variations between the different Model types. In this example the employed models resulted in generated wedges of varying characteristics. For example, the BART, Veneziano and Nearest Neighbour generated a greater number of wedges than the Baecher model. DFNs generated using the BART model resulted in larger size wedges while the Veneziano model generated wedges were consistently smaller. This is an im-

portant consideration when assessing the consequences of failure and the potential need for reinforcement.

The need for quality input data is well recognised. This investigation provided greater insights on the variations in input parameters critical in defining wedge volume and occurrence. Smaller trace length with constant intensity results in a lower number of wedges, smaller in size and reduced probability of occurrence. Larger intensity with constant size distribution results in more wedges but with a similar wedge size distribution. The number of wedges produced for a given length of slope crest is strongly influenced by fracture intensity.

The use of integrated DFN-LEA approaches provides an extremely powerful tool for the analysis and design of bench slopes in open pit mines. The impact of the choice of different DFN generators should be acknowledged and taken into consideration. Failing to do so can potentially lead to misleading interpretation of the results of any undertaken analyses.

## Acknowledgements

The authors would like to acknowledge the financial support of the Natural Science and Engineering Research Council of Canada.

## References

- Baecher G B, Lanney N A, Einstein H H, 1978. Statistical description of rock properties and sampling. Proceedings of the 18th U.S. Symposium on Rock Mechanics, 5C1-8.
- Dershowitz, W.S. and Herda H.H. 1992. Interpretation of fracture spacing and intensity. Proceedings of the 33rd U.S. Rock Mech. Symposium, Santa Fe, New Mexico. pp. 757-766.
- Dershowitz, W.S. and Carvalho, J. 1996. Key-block tunnel stability analysis using realistic fracture patterns. North American Rock Mechanics Symposium, Montreal. (Aubertin et al. eds), pp. 1747-1751.
- Dershowitz W S, Lee G, Geier J, Foxford T, LaPointe P, Thomas A, 1998. FracMan Version 2.6 Interactive Discrete Feature data Analysis, Geometric Modeling, and Exploration Simulation, user documentation, Report 923-1089, Golder Associates Inc, Seattle, Washington.
- Elmo, D., Liu, Y. and Rogers, S. 2014. Principles of discrete fracture network modelling for geotechnical applications. International Discrete Fracture Engineering Conference, DFNE 2014 – 238.
- Elmouttie, M.K. and Poropat, G.V. 2011. Uncertainty Propagation in Structural Modeling Slope Stability 2011: International Symposium on Rock Slope Stability in Open Pit Mining and Civil Engineering, Vancouver, Canada.
- Fisher, N.I., Lewis, T. and Embleton, B.J.J. 1993. Statistical analysis of spherical data. Paperback ed. 1993: Cambridge University Press.
- Geier, J.E., K. Lee, and W.S. Dershowitz, 1988. Field Validation of Conceptual Models for Fracture Geometry," paper H12A-II presented at the American Geophysical Union 1988 Fall Meeting.
- Guest, A. and J. Read 2009. Geotechnical Model. Chapter 7 in Guidelines for Open Pit slope Design. CRC Press, pp. 201-211.
- Grenon, M., Landry, A., Hadjigeorgiou J. and Lajoie, P.J. 2017. Discrete Fracture Network based drift stability at the Éléonore mine. Mining Technology: Transactions of the Institutions of Mining and Metallurgy: Section A, Vol 126, No 1, pp. 22-33.
- Grenon, M and Hadjigeorgiou, J. 2018. *Fracture-SG: a fracture system generator software package*, version 2.25. Quebec City, Canada.
- Grenon, M. and Hadjigeorgiou, J. 2012. Applications of Fracture System Models (FSM) in mining and civil rock engineering design. *International Journal of Mining, Reclamation and Environment*, 26 (1), 55-73.
- Grenon, M. and Hadjigeorgiou, J. 2008. Design of road cuts susceptible to wedge failures using fracture system modelling. *Engineering Geology*, 96, 78-93.
- Grenon, M. and Hadjigeorgiou, J. 2018. Fracture-SL. A Fracture System Based Rock Slope Wedge Stability Analysis Software Package, Version 1.41. Quebec City, Canada.
- Hadjigeorgiou, J. 2012. Where do the data come from? *Mining Technology*, 121 (4), 236-247.
- Jing, L. (2003). A review of techniques, advances and outstanding issues in numerical modelling for rock mechanics and rock engineering. *International Journal of Rock Mechanics and Mining Sciences*, 40(3), 283-353.
- Mathis, J.I. 2016. Structural domain determination – practicality and pitfalls. APSSIM 2016, Brisbane, Australia, pp.203-212.
- Mathis, J.I. 2014. Bench Face Angle Distributions – The Requirement for DFN Analysis. International Discrete Fracture Engineering Conference DFNE 2014 – 105.
- Staub, I., Fredriksson, A. and Outters, N. 2002. *Strategy for a rock mechanics site descriptive model development and testing of the theoretical approach*, SKB report, no. R-02-02, prepared for Golder Associates AB, Stockholm.
- Veneziano D, 1978. Probabilistic model of joints in rock. Unpublished manuscript, Massachusetts Institute of Technology, Cambridge, Massachusetts.
- Zhang, L. and Einstein, H.H. 1998. Estimating the mean trace length of rock discontinuities, *Rock Mechanics and Rock Engineering*, 31(4), 217-235.

Recibido: julio 2019

Revisado: noviembre 2019

Aceptado: enero 2020

Publicado: marzo 2021